Silicon nanomembrane based photonic crystal waveguide array for wavelength-tunable true-time-delay lines

Che-Yun Lin, Harish Subbaraman, Amir Hosseini, Alan X. Wang, Liang Zhu et al.

Additional information on Appl. Phys. Lett.

Silicon nanomembrane based photonic crystal waveguide array for wavelength-tunable true-time-delay lines

Che-Yun Lin,[1] Harish Subbaraman,[2] Amir Hosseini,[2] Alan X. Wang,[3] Liang Zhu,[1] and Ray T. Chen[1,a]

[1]*The University of Texas at Austin, 10100 Burnet Rd, Bldg160 MER, Austin, Texas 78759, USA*
[2]*Omega Optics, Inc., Austin, Texas 78759, USA*
[3]*Oregon State University, Corvallis, Oregon 97331, USA*

We demonstrate a four-channel on-chip true-time-delay module based on a photonic crystal waveguide array. Using the photonic crystal taper to minimize the coupling loss, the delay lines with 1–3 mm long photonic crystal waveguides can operate up to a group index $n_g \sim 23$ without significant loss. The large group velocity dispersion enables continuous and wavelength-tunable time delays. Measurements show a highly linear phase-frequency relation, highest time delay up to 216.7 ps, and large tuning ranges of 58.28 ps, 115.74 ps, and 194.16 ps for 1–3 mm delay lines. The chip-scale true-time-delay module occupies only 0.18 mm^2 area and can provide $\pm 44.38^\circ$ steering for an X-band phased-array-antenna. © 2012 American Institute of Physics. [http://dx.doi.org/10.1063/1.4739003]

Photonic crystal waveguides (PCWs) offer strong optical confinement, slow light enhanced interactions, and strong dispersions. These properties enable realization of many miniaturized and highly efficient devices such as hybrid silicon modulators,[1–3] optical switches,[4] on-chip environmental sensors for underground water pollution detection,[5] and gas sensors for green house gas detection.[6] Recent studies have shown that PCWs can also be used to build optical delay lines.[7,8] However, much of the reports in PCW delay lines have been focused on a single delay line rather than building a chip integrated module. The high dispersion and slow-light PCWs will greatly benefit the development of lightweight and compact systems. Specifically, for applications requiring strict control on payload, such as phased array antenna (PAA) systems[9] in air-borne platforms, such miniaturized systems can enhance functionality while maintaining a minimum form factor. It is well known that photonic true-time-delay (TTD) systems enable broadband operation of PAA due to their inherent characteristic of providing a linear response of phase-frequency relationship across the entire operating bandwidth of the radio-frequency (RF) signal.[10] Furthermore, utilization of PCW TTDs can offer significant reduction in device footprint when operating in the high group index region. A TTD module based on PCW devices shall provide large bandwidth, small footprint, and large tunable time delay.

In this paper, we explore the utilization of a slow-light PCW for application in an X-Band TTD module. A broadband PAA with large steering angle and high directivity requires hundreds or even thousands of radiating elements. A TTD module with large and tunable time delay is required to control the phase of each radiating elements. To create large time delay, PCWs with lengths in mm range are often required. However, the large insertion loss of PCWs can be a prohibitive factor for building such long-length TTD devices. While the propagation loss can be minimized with better etch processes and post-etching oxidation treatment,[11] minimizing coupling loss requires a special design to achieve a

better mode matching at the strip waveguide-PCW interface. Previous demonstrations have achieved 80 ps time delay with a 4 mm long PCW when operated at group index $n_g = 12.5$.[8] In the work reported herein, we use a photonic crystal waveguide taper[12] to minimize coupling loss, which allows the delay lines to operate at a much higher group index that delivers much higher delay time with shorter physical length. Using the four-channel PCW array integrated with a 1×4 multimode interference (MMI) coupler, we experimentally demonstrate the first PCW-based chip-scale integrated TTD module with three continuously tunable true-time-delays covering the ranges of (6.72,65), (10.56,126.3), and (22.54,216.7) ps. The highest group index that we can perform phase-frequency measurement is ~ 23, which is calculated from the maximum time delay (216.7 ps) measured in 3 mm PCW.

The micrograph of the PCW TTD module is shown in Fig. 1(a). The optical input power is uniformly divided into four channels using a 1×4 MMI beam splitter, which has a width and length of 16 μm and 117.7 μm, respectively. The input and output access waveguides widths are 2.5 μm on a 230 nm silicon nanomembrane on a silicon-on-insulator (SOI) wafer, which has been optimized for high MMI performance.[13] Each channel consists of carefully chosen lengths of silicon strip waveguides and PCWs,[12] such that at any given wavelength within the bandwidth of interest, a constant time delay difference is setup between adjacent channels. Channel-1 contains a 5 mm-long silicon strip waveguide and no PCW, and is chosen as a reference line. Channels-2, 3, and 4 contain 4 mm, 3 mm, and 2 mm silicon strip waveguides and 1 mm, 2 mm, and 3 mm-long PCWs, respectively, with identical PCW parameters. When the operating wavelength λ is tuned, this configuration creates proportional relative time delay 0, τ, 2τ, and 3τ in channels-1–4, respectively. Note that since a different τ_i time delay difference is achieved for different tuning wavelength λ_i, the time delay profiles can provide appropriate phase distribution at the output for operation in a PAA. Scanning electron micrographs of the 1×4 MMI and the waveguide splitting

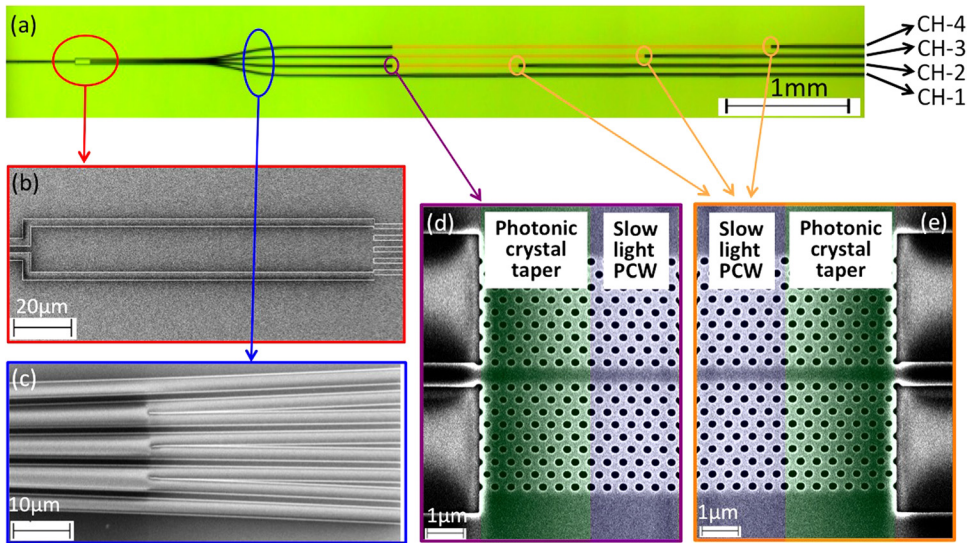a)Electronic mail: raychen@uts.cc.utexas.edu.

FIG. 1. (a) Microscope picture of the TTD beamformer based on a 1*4 MMI and PCWs. (b) SEM picture of the enlarged view of the 1*4 MMI power splitter. (c) Enlarged view of the S-bends that increase the waveguide separations. (d) and (e) SEM pictures of the PCW region containing photonic crystal taper and slow light PCW region.

section for four channels are shown in Figs. 1(b) and 1(c), respectively. The enlarged view of the slow light PCWs and the PCW taper regions are shown in Figs. 1(d) and 1(e), respectively.

In our design, the lattice constant (a), hole diameter (d), and slab thickness (h) of the W1 PCWs are chosen as 405 nm, 190 nm, and 230 nm, respectively, so that the PCWs support a guided mode covering 1533–1573 nm. Detailed design parameters are covered in our previous work.[12] To minimize the coupling loss into the slow light PCW, we utilize two photonic crystal tapers at the strip-PCW interfaces.[12] These structures significantly improve the matching of the two different waveguide modes and reduce coupling loss. Such a design enables operation in the high-group index region near the band-edge, which gives much larger delay time and faster tuning based on wavelength tuning.

The on-chip TTD module is fabricated on a Unibond SOI wafer with a 250 nm top silicon layer and a 3 μm buried oxide (BOX) layer. First, a 45 nm of thermal oxide is thermally grown as an etching mask for pattern transfer. Then, MMI power splitter, PCWs, photonic crystal tapers, and strip waveguides are patterned in one step with a JEOL JBX-6000FS electron-beam lithography system followed by reactive ion etching.

The TTD module is tested on a Newport 8-axis precision automated alignment station, which has a 10 nm horizontal alignment accuracy and 5 nm vertical alignment accuracy. In order to measure the output characteristics of the fabricated device, light from a broadband source is TE polarized and coupled to the TTD module through a polarization maintaining lensed fiber. The output signal from the TTD module is collected using single mode lensed fibers. Transmission spectra of the channels containing PCWs were also characterized to identify the transmission bands of the PCWs experimentally. Note that the measurement data were taken from integrated devices, i.e., the transmission through MMI and PCWs. Transmission spectra for channel-2–4 are shown in Fig. 2, which clearly show overlapping transmission bands from 1533 nm to 1573 nm. Each set of data is composed of 1200 data points to ensure good accuracy, and the results for each of the channels from 2 to 4 were normalized to the

transmission of the strip waveguide channel. The coupling loss of PCWs is significantly reduced due to the implementation of PCW tapers. The highest transmission point is −2.68 dB for channel-2, which contains 1 mm long PCW. The increasingly large fluctuation in the transmission spectra for longer PCWs channels is mainly due to the propagation loss from the fabrication related imperfections in the PCWs.

The schematic of the measurement setup is shown in Fig. 3(a). In order to measure the time delay from the TTD lines, a X-band (8-12 GHz) RF signal from an HP8510C vector network analyzer (VNA) is modulated onto an optical carrier from a tunable continuous wave laser by a LiNbO$_3$ modulator. The output of the modulator is coupled to the on-chip TTD module using the same method used to characterize the transmission spectra of TTD channels. A photodetector (PD) covering the X-band frequency range is used to convert the modulated optical signal to an electrical signal, which is then amplified using an X-band RF amplifier and fed back to the network analyzer. The time delay of the RF signal achieved in the TTD module for a given wavelength is obtained from the phase-frequency measurement using a VNA. The time delay from strip waveguide channel (channel-1) is subtracted from the measurement results in channel-2–4 to show the relative time delays in delay lines
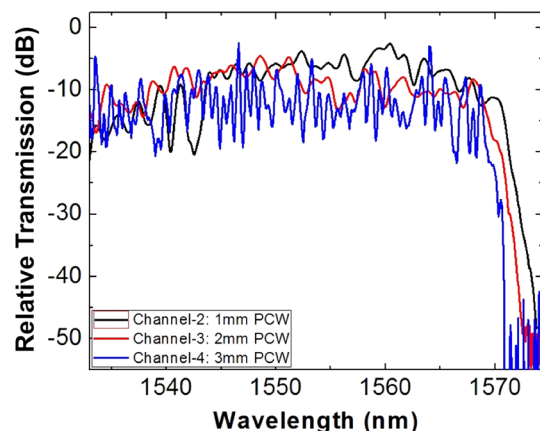

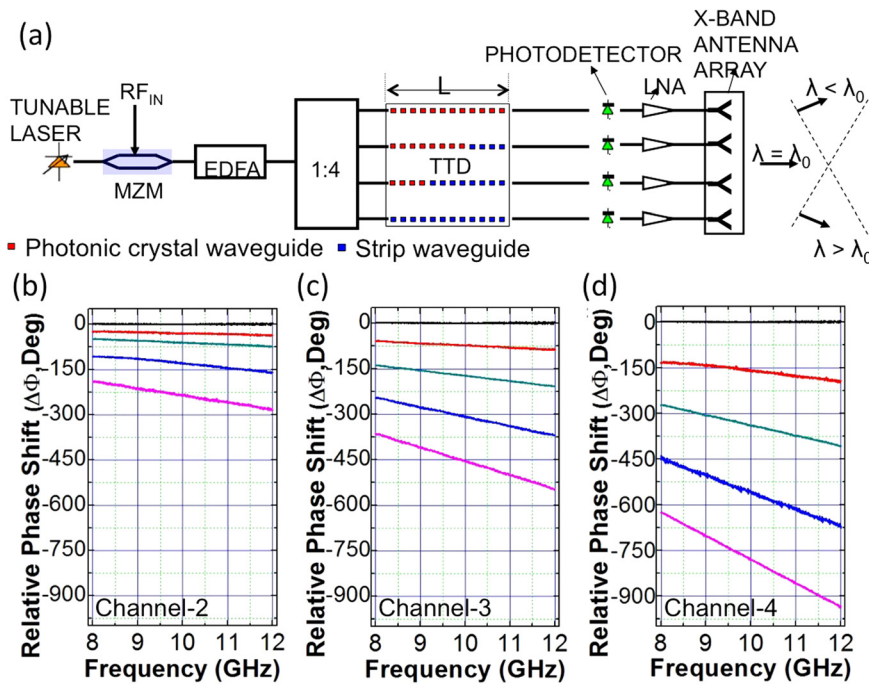FIG. 2. Transmission spectra of the channels containing 1–3 mm PCWs.

FIG. 3. (a) A schematic of the measurement setup of a PCW-based TTD module. Measurement results of phase vs. frequency relation for (b) channel-2, (c) channel-3, and (d) channel-4. Measurement results were normalized to the strip waveguide (channel-1). The horizontal line (black) in (b), (c), and (d) represents the normalized phase shift of channel-1. From top to bottom, each color line represents the measurements performed at $\lambda = 1548$ nm, 1552 nm, 1562 nm, and 1568 nm, respectively.

that contain PCWs. Due to the strong fluctuation in transmission spectra below 1545 nm and above 1572 nm, time delay measurements were only performed between 1545 nm and 1572 nm to avoid strong optical loss. The wavelength of the optical carrier is then tuned continuously from 1545 nm to 1572 nm. Because the group index increases with wavelength, the time delay also increases with wavelength accordingly. This phenomenon is shown in the increasing slopes in Figs. 3(b)–3(d). Highly linear phase-frequency relation is seen in all the channels, which clearly shows constant time delay for all frequencies-the signature of true-time-delay. This characteristic is critical to have a wide band phased array antenna without beam squint effect covering the whole X-band (8 to 12.5 GHz).[14] The time delay (τ) in the PCWs is derived from a linear regression fit following the relation $\tau = \Delta\Phi/\Delta\omega$, where $\Delta\Phi$ represents the changes of phase in the measurement frequency range $\Delta\omega$. Accordingly, the maximum time delays obtained are 65 ps, 126.3 ps, and 216.7 ps for channels-2, 3, and 4, respectively. The maximum relative time delay we measured (216.7 ps) corresponds to a group index $\sim$23, the highest group index we

can operate our delay lines under constraints such as propagation loss and pulse distortion related to strong dispersion in high group index mode.

The wavelength-tunable time delay results are summarized in Fig. 4. When external tunable delay lines are used to offset the time delay difference between adjacent delay lines, this TTD module can provide a steering angle from $-44.38°$ to $44.38°$ if wavelength is tuned from a central wavelength $\lambda_0 = 1558.5$ nm for an X-Band PAA with inter-element spacing of 1.25 cm. Further system demonstration containing a real X-band phased array antenna is under investigation and further results will be presented in the near future.

In conclusion, we experimentally demonstrate a chip-scale four-channel TTD module based on slow light photonic crystal waveguides. The implementation of photonic crystal waveguide tapers enables device operation in the high group index region near the band edge, thus allowing access to much larger time delays. The integrated TTD module offers continuous wavelength tunable time delays up to 216.7 ps for a PCW with a length of 3 mm. Further optimization of the interfaces between MMI and PCWs can lead to lower optical loss, and better signal quality. The utilization of even longer PCW channels can cover time delays up to 1 ns, which can accommodate more delay line channels and give better directivity. Such a compact device can be implemented in a broadband PAA system in order to achieve large steering angles within the whole X-band.
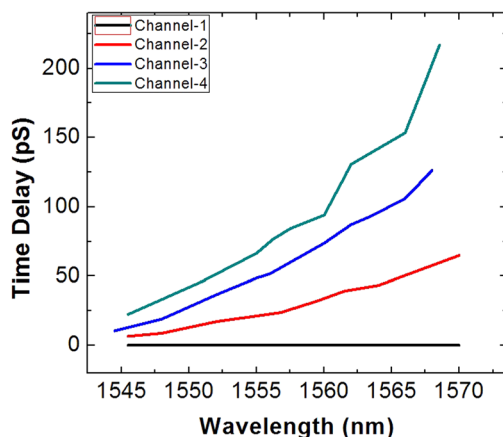
FIG. 4. Wavelength-tunable time delay for all four channels.

[1]X. Wang, C.-Y. Lin, S. Chakravarty, J. Luo, A. K. Y. Jen, and R. T. Chen, Opt. Lett. **36**, 882 (2011).
[2]C.-Y. Lin, X. Wang, S. Chakravarty, B. S. Lee, W. Lai, J. Luo, A. K.-Y. Jen, and R. T. Chen, Appl. Phys. Lett. **97**, 093304 (2010).

[3]J.-M. Brosi, C. Koos, L. C. Andreani, M. Waldow, J. Leuthold, and W. Freude, Opt. Express **16**, 4177 (2008).

[4]D. M. Beggs, T. P. White, L. O'Faolain, and T. F. Krauss, Opt. Lett. **33**, 147 (2008).

[5]W.-C. Lai, S. Chakravarty, X. Wang, C. Lin, and R. T. Chen, Appl. Phys. Lett. **98**, 023304 (2011).

[6]W.-C. Lai, S. Chakravarty, X. Wang, C. Lin, and R. T. Chen, Opt. Lett. **36**, 984 (2011).

[7]T. Baba, Nat. Photonics **2**, 465 (2008).

[8]A. Melloni, A. Canciamilla, C. Ferrari, F. Morichetti, L. O'Faolain, T. F. Krauss, R. De La Rue, A. Samarelli, and M. Sorel, IEEE Photonics J. **2**, 181 (2010).

[9]H. Subbaraman, M. Y. Chen, and R. T. Chen, J. Lightwave Technol. **26**, 2803 (2008).

[10]I. Frigyes and A. J. Seeds, IEEE Trans. Microwave Theory Tech. **43**, 2378 (1995).

[11]L. Ofaolain, X. Yuan, D. McIntyre, S. Thoms, H. Chong, R. M. De La Rue, and T. F. Krauss, Electron. Lett. **42**, 1454 (2006).

[12]C.-Y. Lin, X. Wang, S. Chakravarty, B. S. Lee, W.-C. Lai, and R. T. Chen, Appl. Phys. Lett. **97**, 183302 (2010).

[13]A. Hosseini, H. Subbaraman, D. Kwong, Y. Zhang, and R. T. Chen, Opt. Lett. **35**, 2864 (2010).

[14]H. Subbaraman, M. Y. Chen, and R. T. Chen, Appl. Opt. **47**, 6448 (2008).